

# Analysis of excitation of the 630.0 nm airglow during a heating experiment in Tromsø on February 16, 1999.

T. Sergienko<sup>1,\*</sup>, B. Gustavsson<sup>2</sup>, Å. Steen<sup>2</sup>, U. Brändström<sup>2</sup>, M. Rietveld<sup>3</sup>, T.B. Leyser<sup>4</sup>, and F. Honary<sup>5</sup>

<sup>1</sup>Polar Geophysical Institute, Russian Academy of Sciences, Apatity, Russia.

<sup>2</sup>Swedish Institute of Space Physics, Kiruna Division, Sweden

<sup>3</sup>European Incoherent Scatter Association, Ramfjordboth, Norway

<sup>4</sup>Swedish Institute of Space Physics, Uppsala Division, Sweden

<sup>5</sup>Communications Research Center, Lancaster University, UK

\* Present address Swedish Institute of Space Physics, Kiruna Division, Sweden

Received 2000 – Accepted 2000

**Abstract.** During an ionospheric heating experiment in Tromsø during February 1999, artificial 630.0 nm airglow enhancements have been observed by the auroral large imaging system (ALIS). The airglow enhancements took place in the F region of the ionosphere near the heating wave reflection point. Two possible mechanisms are proposed for the explanation of this phenomenon. The first is the excitation of the  $O(^1D)$  state by the energetic electrons from the tail of the artificially heated thermal electron gas, and the second is the excitation of this state by the plasma instability accelerated electrons. The detailed spatial and temporal characteristics of the red line airglow are obtained from the ALIS measurements. An analysis of these characteristics based on the models of thermal response of the ionosphere and the atmospheric optical emissions allows us to draw conclusions about the mechanism of the interaction between the heating radio wave and the ionospheric plasma.

## 1 Introduction

During ionospheric disturbances induced by powerful electromagnetic waves transmitted from the ground, enhanced airglow may be formed. Such artificial airglow has been clearly observed on many occasions at middle latitudes, at Arecibo (Sipler and Biondi, 1972; Carlson et al., 1982; Bernhardt et al., 1989), at Moscow (Adeishvili et al., 1978), at Sura (Bernhardt et al., 1991), and possibly at the auroral latitude of Tromsø (Stubbe et al., 1982; Henriksen et al., 1984; Sergienko et al., 1997). Generally the artificial airglow is attributed to the emission of the “red line” of the atomic oxygen at the wavelength of 630.0 nm. This emission is produced in radiative transitions from the electronically excited  $O(^1D)$  state to the  $O(^3P)$  ground state of atomic oxygen. The metastable  $O(^1D)$  state can be formed in the ionosphere by energetic electrons with energy

higher than 1.96 eV as well as by different chemical reactions. To explain the observed artificial airglow two possible mechanisms were suggested. First is the production of high-energy suprathermal electrons due to acceleration by Langmuir waves in the region near the reflection point of the heating wave (Bernhardt et al., 1989; Meltz and Perkins, 1974; Gordon and Carlson, 1974; Gurevich et al., 1985). Another process is the electron heating due to absorption of the HF wave. In this process the electron temperature increases, while the energy distribution remains essentially Maxwellian (Biondi et al., 1970; Mantas, 1994; Mantas and Carlson, 1996; Gurevich and Milikh, 1997). There are no experimental data either to support or refute one of these mechanisms.

In February and March, 1999, a series of experiments were carried out, attempting to produce enhanced airglow with the EISCAT Heating facility, and detect it with the Auroral Large Imaging System (ALIS) (Steen and Brändström, 1993). As noted by Stubbe et al. (1982) such experiments require, a sufficiently high ionosphere critical frequency, dark and clear skies, no aurora activity and a low or at least stable natural airglow background. These criteria were fulfilled on February 16 and 21, 1999 and on March 15-17, 1999. During some of these events the EISCAT-UHF radar measured ionospheric plasma parameters such as the electron density and the electron and ion temperatures. In this paper we will consider the analysis of the events on February 16. A detailed description of the instrument and the optical data for this event were presented in Brändström et al. (1999).

Particular attention in this paper is devoted to the aeronomic aspects of the observed artificial airglow. The first paper concerning the airglow intensity variation due to ionospheric modification by powerful radio waves was that of Biondi et al. (1970). The authors analyzing the data of the heating experiment at Platteville concluded that the ‘red line’ intensity variation can be explained by changing the rate of the dissociative recombination of  $O_2^+$  ions and electrons, which correlates with heating of ionospheric electrons. They showed that the intensity of the 630.0 nm

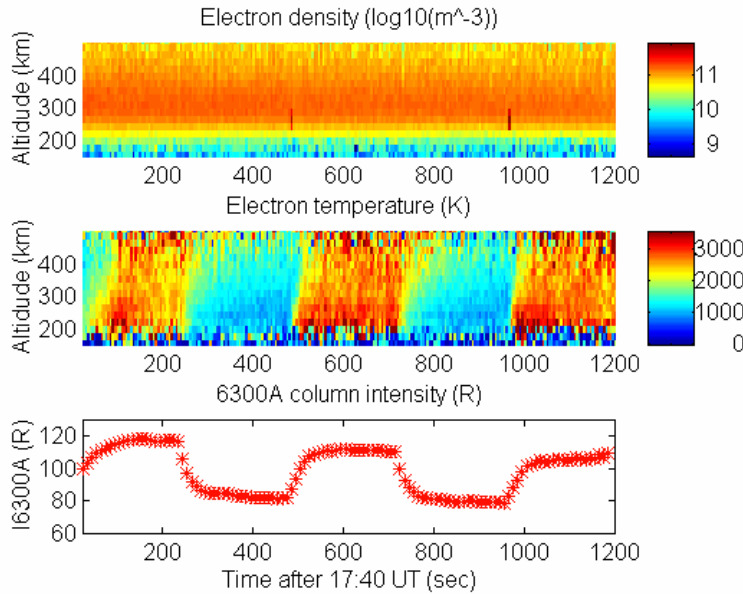


**Fig. 1.** The ionospheric electron density (top panel), electron temperature (middle panel) versus altitudes measured with the EISCAT UHF incoherent scatter radar, and the 630.0 nm column emission intensity measured with ALIS. The measurements were made during the ionosphere heating experiments February 16, 1999 with EISCAT heating facility.

emission initially decreases when the electron temperature is raised and a sudden decrease in electron temperature leads to a momentary increase in airglow intensity after the transmitter is switched off. However, in subsequent heating experiments obvious enhancement of the 630.0 nm airglow has been observed. Starting from the paper by Sipler and Biondi (1972), the artificially enhanced airglow has been attributed to excitation of the oxygen atoms by fast electrons heated due to either plasma instability acceleration or heating of the ionospheric plasma. Since then all subsequent authors analyzing the heating induced 633.0 nm intensity variations have assumed only the impact mechanism for excitation of the  $O(^1D)$  state in their aeronomic models (Sipler et al., 1974; Haslett and Megill, 1974; Bernhardt et al. 1989; Mantas, 1994; Mantas and Carlson, 1996; Gurevich and Milikh, 1997). However, the experimental data from the ionospheric heating experiments show that the 630.0 nm intensity variations do not exceed the background intensity (that was usually close to 80 R) by more than 50%. At night time the major channel for the  $O(^1D)$  state production at the F region altitudes is the dissociative recombination of  $O_2^+$  ions with electrons. The recombination coefficient varies with electron temperature as  $T_e^{-0.7}$ , and the background intensity can be changed significantly during the HF radio wave ionospheric modification. Thus, for correct analysis of the optical effect it is necessary to use a more complete aeronomic model.

## 2 Data and model

Figure 1 presents the EISCAT UHF radar and optical data obtained during the heating experiment at Tromsø on February, 16, for the time interval 17:40-18:00 UT. The top and middle panels show the number density and

temperature of the ionospheric electrons, and the bottom panel shows the airglow intensity observed by the ALIS station. The airglow intensity is the column intensity of the 630.0 nm emission at the same point for each airglow image. This point was chosen so as to be close to the region of maximum intensity enhancement which varied with time as well as from one cycle to another. The EISCAT measurements demonstrate a large increase of the electron temperature during the “heating on” period. A strong correlation between the temperature and the airglow variation is apparent. The EISCAT data show that there is no noticeable heating effects on the electron density. However, the natural decrease of ionospheric plasma density is clearly seen. The optical data demonstrate a decrease of the airglow background if we assume that the 630.0 nm intensity reaches the natural background level at the end of each interval when the transmitter was turned off.

In our analyses we use the  $O(^1D)$  state excitation scheme described by Solomon et al. (1987). This model involves a number of the chemical reactions between the ionized and neutral atmospheric species, the behavior of which can only be inferred from the model calculation. Our model produces the altitude distribution (along magnetic field line) of the density of 7 ions ( $N_2^+$ ,  $O_2^+$ ,  $O^+(^4S, ^2D, ^2P)$ ,  $NO^+$ ,  $N^+$ ), 6 minor neutral thermospheric species ( $O(^1D, ^1S)$ ,  $N(^4S, ^2D, ^2P)$ ,  $NO$ ) and electrons; electron and ion temperatures, and ion velocity. This ionospheric-thermospheric model is based on solving the time-dependent one dimensional continuity equations for each species, the motion equation for ions, and the heat conduction equation for electrons and ions. Input parameters of the model are the neutral composition and temperature (MSIS90 thermospheric model (Hedin, 1991)), the ultraviolet solar flux, and the characteristics of the

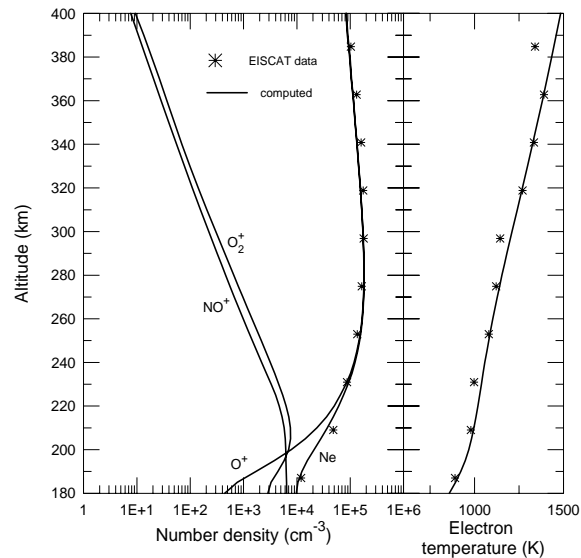


**Fig. 2.** The altitude profiles of the ion and electron concentrations and electron temperature used in calculation as the initial conditions. Asterisks give the electron density and temperature measured with EISCAT UHF radar at 17:38 UT.

precipitation particle flux. A detailed description of the model is not possible in this paper and will be presented elsewhere. To obtain the initial conditions at 17:40 UT the model was first run for 5 hours under the geophysical conditions typical for February, 16 1999. The number densities of three ions, electrons and electron temperature calculated for the time of 17:40 UT are presented in Fig. 2. The measured electron density and temperature taken from the EISCAT data are shown for comparison.

Although the final absolute intensity calibrations of the ALIS stations are not available, in Fig. 1 the 630.0 nm column intensity is given in Rayleighs. The absolute values of the emission intensities were obtained by normalization of the experimental background intensity (the emission intensity at the end of “heating off” period for each heating pulse) to the background level of the 630.0 nm intensity calculated with our model. The absolute values of the emission intensity obtained in such way are in satisfactory agreement with preliminary estimations presented by Brändström et al. (1999).

### 3 Results and discussion

A mechanism for the enhancement of the 630.0 nm airglow that has been widely accepted is the excitation of oxygen atoms to the  $O(^1D)$  state by ionospheric electrons energized by powerful HF radio waves to an energy of more than 1.96 eV. There are two quite different theoretical predictions of the possible mechanisms of such electron energization. One of these is the production of suprathermal electrons due to acceleration by Langmuir waves in the region of the ionosphere, where most of the heating radio wave energy is absorbed. This mechanism was analyzed by many authors

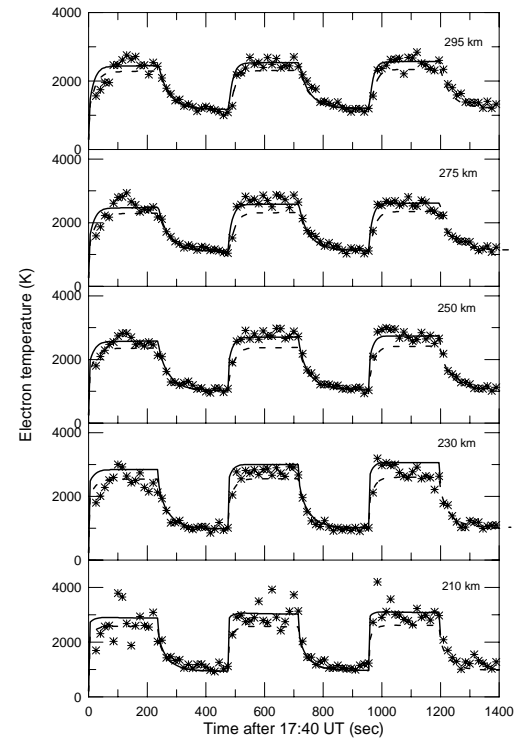


**Fig. 3.** Time variation of electron temperature at fixed altitudes. Asterisks give the EISCAT UHF radar measurements. Solid and dashed lines are modeled temperatures calculated for the different values of the electron heating source

(Meltz and Perkins, 1974; Gordon and Carlson, 1974, Gurevich et al., 1985, Bernhardt et al., 1989) and has been widely adopted as a major source of the observed artificial airglow. Another mechanism for electron energization considered in papers by Mantas and Carlson (1996) and Gurevich and Milikh (1997) is electron heating due to the HF pump wave absorption. In this process the electron temperature increases, while the energy distribution remains essentially Maxwellian. In this section we consider both mechanisms and compare the calculated results with observations.

According to Gurevich and Milikh (1997) significant local electron heating can occur inside striations elongated along the geomagnetic field which are generated by powerful radio waves in the upper ionosphere. The region of abnormal electron heating is located lower than reflection point of the HF radio wave but above upper hybrid resonance level. The extent of this region is approximately 2-4 km for the HF radio wave reflection altitude of 250-300 km. According to the EISCAT data, the reflection altitude varied from 235 km to 250 km during the time interval 17:40 – 18:00 UT. Thus we assumed in our calculations that the altitude of the heating source is below 240 km. We have used the EISCAT measurements of electron temperature to estimate the position and magnitude of the heating source. For this we adjusted the magnitude of the heating source in our model so that the calculation gives

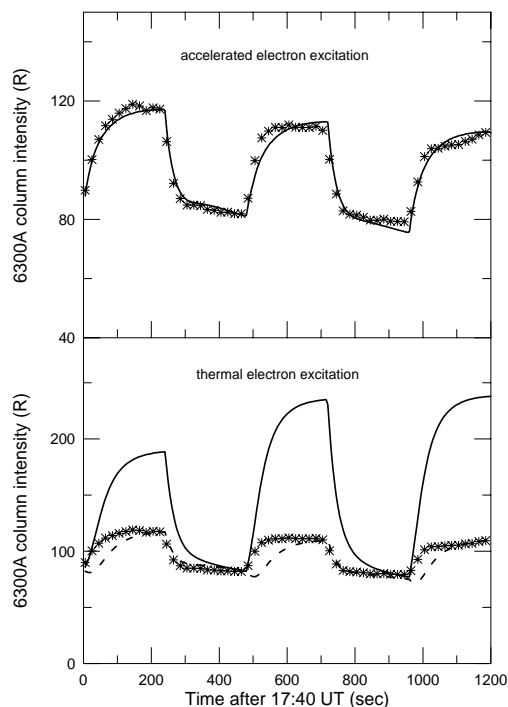


**Fig. 4.** Time variation of the column 630.0 nm intensity. Asterisks give the data of ALIS. The top panel shows the modeled emission intensity calculated assuming the acceleration of ionospheric electrons by Langmuir waves in the region of the heating wave reflection point. The bottom panel shows calculated results obtained assuming the abnormal electron heating inside radio wave generated striation. Solid and dashed lines correspond to various intensity of the electron heating source.

the best fit to the observed time behavior of the electron temperature at all altitudes. Following this procedure, we determined that the position and the magnitude of the heating source should be 220 km and  $6 \cdot 10^4$  eVcm<sup>-3</sup>sec<sup>-1</sup>. Fitting the model to the data, presented in Fig. 3, demonstrates a good agreement between the measured (asterisk) and calculated (solid line) temperatures. Fig. 4 presents the column intensity of the “red line”. The bottom panel of this figure shows the emission intensity calculated with our model assuming the thermal mechanism of the ionospheric electron energization. The solid line gives the airglow intensity calculated with the heating source derived from the EISCAT data. It is clearly seen that the thermal excitation mechanism leads to large overestimates of the calculated airglow intensities.

We have tried to fit the magnitude of the heating source such that the calculated and measured airglow intensities agree better. The dashed line in the bottom panel of Fig. 4 gives the 630.0 nm column intensity resulting from this fit. The volume heating rate for this calculation is  $4 \cdot 10^4$  eVcm<sup>-3</sup>sec<sup>-1</sup>. The electron temperature calculated for this case is shown in Fig. 3 by dashed lines. There are significant differences between the modelled and observed data for both the electron temperature and the airglow intensity. These differences are especially noticeable for the optical

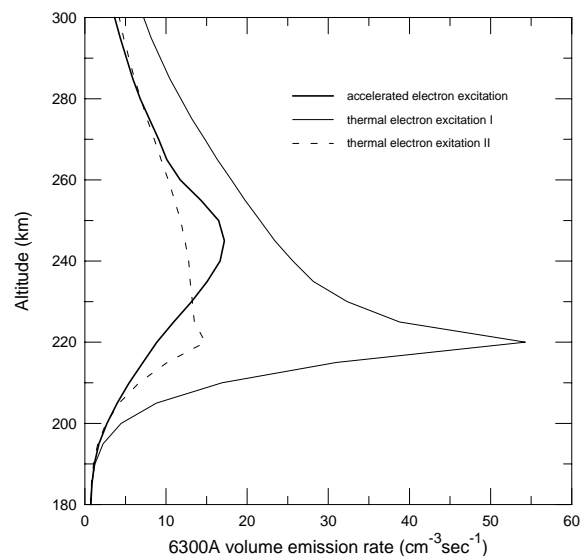


**Fig. 5.** Disturbed altitude profiles of the 630.0 nm volume emission rate calculated for different mechanisms of the interaction of the heating HF radio waves with the ionospheric plasma.

data. A very slow increase of the calculated value in comparison with the measured ones is obvious. The explanation of such behavior of the computed intensity is a competition of different excitation mechanisms of the  $O(^1D)$  state involved in our model. The main excitation mechanism of the atomic oxygen  $O(^1D)$  state in the night ionosphere is the dissociative recombination reaction between the molecular oxygen ions and electrons. The rate coefficient for this reaction is proportional to  $T_e^{-0.7}$ . Therefore the 630.0 nm emission intensity should increase more slowly than the electron temperature, and this lag should exist for all realistic processes of ionospheric electron heating. However, the experimental data does not demonstrate a noticeable time delay between the electron temperature and the airglow.

There is another discrepancy between the experimental and modelled optical data that exists if the abnormal electron heating is accepted as the possible mechanism for the electron energization. The enhanced airglow was detected by three ALIS stations simultaneously, and triangulation of the height of the airglow maximum is possible. The altitude of the maximum 630.0 nm intensity is found to be approximately 240 km. The altitude profiles of the volume emission rate calculated with our model are shown in Fig. 5. The light solid and dashed lines give the emission rate profiles corresponding to the volume heating rates of  $6 \cdot 10^4$  and  $4 \cdot 10^4$  eVcm<sup>-3</sup>sec<sup>-1</sup>, respectively. The altitude of the maximum of the calculated 630.0 nm emission rate is above 220 km. This height is very close to the altitude of the maximum enhanced electron temperature and lies significantly lower than the observed airglow intensity maximum.

Thus, our calculations show that the assumption of abnormal electron heating generated by powerful radio

wave leads to a possible explanation of the observed variation of the electron temperature, but can not account for the measured airglow variations. A possible explanation of this discrepancy could be the assumption that the energy distribution of ionospheric electrons with energies more than 2 eV is strongly non-Maxwellian. Such an electron distribution can be formed due to the inelastic electron collisions with the neutral atmospheric gases. As a result of these energy losses the number of the electrons with energy more than the excitation threshold of  $O(^1D)$  state could be insufficient to generate the observed airglow. Therefore another mechanism forming the artificial airglow is needed.

As an alternative process leading to airglow enhancement during ionospheric modification by powerful HF radio waves, we consider the acceleration of electrons by Langmuir turbulence. Following the analysis of Bernhardt et al. (1989), we assume that interaction of the HF radio wave with the ionospheric plasma forms an isotropic flux of suprathermal electrons with a uniform energy distribution in the energy range 3 – 10 eV at the altitude of the heating wave reflection point. To calculate the production rate of the  $O(^1D)$  state by the electron impact we apply the Monte-Carlo model for electron transport into the atmosphere (Ivanov and Sergienko, 1992). The time variation of the 630.0 nm column emission rate calculated for a suprathermal electron flux of  $1.9 \cdot 10^9 \text{ eV}^{-1} \text{ cm}^{-2} \text{ sec}^{-1}$  is plotted in the top panel of Fig. 4. The electron heating mechanism described above is taken into account in this calculation also. The agreement between the measured (asterisk) and calculated (solid line) airglow intensities is good enough. Furthermore the altitude of the maximum intensity of the 6300Å emission obtained by calculation agrees well with the observed height. The altitude profile of the volume emission rate of the “red line” is shown in Fig. 5 (heavy solid line). Thus, it is likely that in the heating experiment on February, 16, the enhanced optical emission is generated due to excitation of the  $^1D$  state of atomic oxygen by suprathermal electrons accelerated by Langmuir wave in the region of the heating radio wave reflection point.

#### 4 Conclusion

An ionospheric-thermospheric model was used for analysis of the EISCAT UHF measurements and the optical data obtained during the ionospheric heating experiments in Tromsø on February 16, 1999. Analysis shows that the ionospheric heating and the enhanced airglow are likely to be generated by different mechanisms of the interaction between the HF radio waves and the ionospheric plasma. Presumably, the electron temperature can be enhanced through abnormal electron heating inside radio wave generated striations, but the enhanced airglow can be formed by fast electrons accelerated by Langmuir waves in the region of the heating wave reflection point.

*Acknowledgements.* The EISCAT Scientific Association is supported by Suomen Akatemia of Finland, Centre National de la Recherche Scientifique of France, Max-Planck-Gesellschaft of Germany, the National

Institute of Polar Research of Japan, Norges Forskningsråd of Norway, Naturvetenskapliga Forskningsrådet of Sweden, and the Particle Physics and Astronomy Research Council of the United Kingdom.

#### References

- Adeishvili, T.G., Gurevich, A.V., Lyakhov, S.B., Managadze, G.G., Milikh, G.M., and Shlyuger, I.S., Ionospheric emission caused by an intense radio wave. *Sov.J.Plasma Phys.*, *4*, 721-726, 1978.
- Bernhardt, P.A., Tepley, C.A., and Duncan, L.M., Airglow enhancements associated with plasma cavities formed during ionospheric heating experiments. *J.Geophys.Res.*, *94*, 9071-9092, 1989.
- Bernhardt P.A., Scales, W.A., Grach, S.M., Keroshtin, A.N., Kotik, D.S., and Polyakov, S.V., Excitation of artificial airglow by high power radio waves from the “Sura” ionospheric heating facility. *Geophys.Res.Lett.*, *18*, 1477-1480, 1991.
- Biondi, A.A., Sipler, D.P., and Hake, R.D., Optical ( $\lambda$ -6300) detection of radio frequency heating of electron in the F region. *J.Geophys.Res.*, *75*, 6421-6424, 1970.
- Brändström, B.U.E., Leyser, T.B., Steen, Å., Rietveld, M.T., Gustavsson, B., Aso, T., and Ejiri, M., Unambiguous evidence of HF pump-enhanced airglow at auroral altitudes. *Geophys.Res.Lett.*, *26*, 3561-3564, 1999.
- Carlson, H.C., Wickwar, V.B., and Mantas, G.P., Observation of fluxes of suprathermal electrons accelerated by HF excited instabilities. *J.Atmos.Terr.Phys.*, *44*, 1089-1100, 1982.
- Gordon, W.E. and Carlson, H.C., Arecibo heating experiments. *Radio Sci.*, *9*, 1041-1047, 1974.
- Gurevich A.V. and Milikh, G.M., Artificial airglow due to modification of the ionosphere by powerful radio waves. *J.Geophys.Res.*, *102*, 389-394, 1997.
- Gurevich, A.V., Dimant, Y.S., Milikh, G.M., and Vaskov, V.V., Multiple acceleration of electrons in the regions of high-power radio-wave reflection in the ionosphere. *J.Atmos.Terr.Phys.*, *47*, 1057-1071, 1985.
- Haslett, J.C. and Megill, L.R., A model of the enhanced airglow excited by RF radiation. *Radio Sci.*, *11*, 1005-1019, 1974.
- Hedin, A.E., Extension of the MSIS thermospheric model into the middle and lower atmosphere. *J.Geophys.Res.*, *96*, 1159-1172, 1991.
- Henriksen, K.M., Stoffregen, W., Lybekk, B., and Steen, Å., Photometer and spectrometer search of the oxygen green and red lines during artificial ionospheric heating in the auroral zones. *Ann.Geophys.*, *2*, 73-76, 1984.
- Ivanov, V.E. and Sergienko, T.I., *Interaction of the auroral electrons with the atmospheric gases. (The Monte-Carlo modeling)*, “Nauka”, St.-Petersburg, 1992.
- Mantas, G.P., Large 6300- Å airglow intensity enhancements observed in ionospheric heating experiments are excited by thermal electrons. *J.Geophys.Res.*, *99*, 8993-9002, 1994.
- Mantas, G.P. and Carlson, H.C., Reinterpretation of the 6300- Å airglow enhancements observed in ionospheric heating experiments based on analysis of Platteville, Colorado, data. *J.Geophys.Res.*, *101*, 195-209, 1996.
- Meltz, G. and Perkins, F.W., Ionospheric modification theory: Past, present, and future. *Radio Sci.*, *9*, 885-888, 1974.
- Sergienko, T., Kornilov, I., Belova, E., Turunen, T., and Manninen, J., Optical effects in the aurora caused by ionospheric HF heating. *J.Atmos.Terr.Phys.*, *59*, 2401-2407, 1997.
- Sipler D.P., and Biondi, M.A., Measurements of  $O(^1D)$  quenching rates in the F region. *J.Geophys.Res.*, *77*, 6202-6212, 1972.
- Sipler D.P., Enemark, E., and Biondi, M.A., 6300- Å intensity variations produced by the Arecibo ionospheric heating experiment. *J.Geophys.Res.*, *79*, 4276-4280, 1974.
- Solomon, S.C., Hays, P.B., and Abreu, V.J., The auroral 6300- Å emission: Observation and modeling. *J.Geophys.Res.*, *93*, 9867-9882, 1988.
- Steen, Å. and Brändström, U., A multi station ground-based imaging system at high latitudes, *STEP International newsletter*, *3*, 11-14, 1993.
- Stubbe, P., Kopka, H., Lauche, H., Rietveld, M.T., Brekke, A., Holt, O., Jones, T.B., Robinson, T., Hedberg, Å., Thide, B., Crochet, M., and Lotz, H.J., Ionospheric modification experiment in northern Scandinavia. *J.Atmos.Terr.Phys.*, *44*, 1025-1041, 1982.